WSRC-MS-2004-00099

Key Words:
Alanate Decomposition
Modeling
Simulation

UNCLASSIFIED

Does Not Contain
Unclassified Controlled
Nuclear Information

A reversible mechanism for sodium alanate: the role of alanes and the catalytic effect of the dopant (U)

by

R. Tom Walters & J. H. Scogin

16 January 2004

A paper for publication in the
Journal of Alloys and Compounds

A reversible mechanism for sodium alanate: the role of alanes and the catalytic effect of the dopant

R. Tom Walters*, J. H. Scogin
Westinghouse Savannah River Company, LLC, Savannah River Technology Center, Aiken, SC 29808

Abstract

We propose a reversible mechanism for sodium alanate. The individual mechanistic reaction steps for the decomposition reaction derive a set of time dependent differential equations that simultaneously produce the evolution plots for each species. These plots reproduce several aspects of in-situ XRD data, as well as the measured relative composition of selected decomposition samples at various extents of reaction. The presence of alanes facilitates both the decomposition and reformation of sodium alanate based on the principle of microscopic reversibility. A major role for the titanium dopant in catalyzed sodium alanate dynamics appears to be alloy formation at the surface of bulk aluminum that facilitates the formation and sorption properties of alanes.

Key words: Hydrogen absorbing materials, Catalysis, Computer Simulations

1. Introduction

The Basic Energy Sciences Workshop on Hydrogen Production, Storage, and Use targeted hydrogen storage as an area in need of fundamental research. “Finding onboard hydrogen storage solutions for transportation applications is one of the major challenges in achieving the hydrogen economy.” [1] The task of providing large capacity, low temperature reversible solid hydrogen storage for mobile applications has focused lately on a class of reducing agents known as alanates. These complex metal hydrides in general offer a higher weight percent hydrogen than rare earth and transition metal hydrides. Notwithstanding the growing body of data concerning alanate hydrogen storage materials, a satisfactory description of the reversible mechanism for sodium alanate does not exist. [2-30]

In 1997, Bogdanovic and Schwickardi found reversible hydrogen content and accelerated kinetics for sodium alanate at temperatures well below the melting point by doping the material with selected transition or rare-earth metals. [12] Soon after that, Zidan et al. and Jensen et al. report further improvements in the sorption kinetics of

sodium alanate using a new synthetic method and a double rare-earth dopant. [14,15] Yet, the reversible mechanism of doped sodium alanate remains a rather novel and somewhat complicated, if not mysterious, process. [19] Paradoxically, the doped reaction proceeds in the solid state accelerated by catalytic amounts of discrete metallic impurities. Upon complete hydrogen evolution, only spatially separated sodium hydride and bulk aluminum metal remain. Rehydrogenation returns the crystalline sodium alanate. The addition of dopants lowers the activation energy but preserves the thermodynamic parameters, which indicates the dopants act as true catalysts. Since the products of the doped (catalyzed) and neat (uncatalyzed) sodium alanate decomposition are the same [16,24], it appears the same mechanism generally applies to both.

The effect of small amounts of transition metals on the reaction dynamics is dramatic: it begs the question how a metal dispersed in the solid matrix of a complex metal hydride alters the dynamics and allows reversible sorption of hydrogen. The purpose of this paper is to provide for the first time a set of reaction steps that together describe a logical mechanism for the thermal decomposition of doped sodium alanate. A branching chain reaction mechanism evolves a set of time dependent differential equations with sodium hydride playing the double role of chain carrier and termination species. When solved simultaneously, these equations produce the evolution plots for each species. We interrogate these plots against the growing body of data now appearing in the scientific literature. Accordingly, the decomposition reactions lead to a set of rehydrogenation reactions based on the presence of AlH_3 alane in both the forward and reverse equation sets. This reversible mechanistic description further suggests the task the titanium dopant performs in the catalyzed sodium alanate dynamics.

2. The Proposed Decomposition Mechanism

On heating neat sodium alanate ($NaAlH_4$) [31], both decomposition and hydrogen evolution occur in two Phases, represented by the two overall stoichiometric equations (1) and (2). [12,18] The proposed decomposition mechanism is a series of reactions that show a simple progression from starting material ($NaAlH_4$) to the known intermediate (Na_3AlH_6) to the final products (NaH and Al). This series of reactions describes the decomposition process for both solid and fused (>180°C) $NaAlH_4$.

$$3NaAlH_4 \rightarrow Na_3AlH_6 + 2Al + 3H_2 \quad (1)$$

$$Na_3AlH_6 \rightarrow 3NaH + Al + 3/2\ H_2 \quad (2)$$

During Phase 1 (equation 1), thermally activated $NaAlH_4$ initially produces NaH and the alane AlH_3 in a rather singular environment of primarily $NaAlH_4$. The NaH can react with $NaAlH_4$ and eventually produce Na_3AlH_6 by another reactive encounter with a second NaH. [3,4,6,7,9] This first consumption of NaH produces a material with the stoichiometry [Na_2AlH_5], a simple addition reaction of NaH with $NaAlH_4$. [9] The brackets signify this “di-sodium” alanate is not yet identified. Nevertheless, this reaction limits the concentration of NaH to a very low level.

As $NaAlH_4$ decomposes, the overwhelmingly large concentration of $NaAlH_4$ inhibits the consumption of [Na_2AlH_5]. As the concentration of $NaAlH_4$ decreases, the reaction of NaH with [Na_2AlH_5] naturally becomes more likely, and the [Na_2AlH_5] species begins to disappear from the system as Na_3AlH_6 grows in. AlH_3 decomposes concurrently, producing hydrogen atoms and bulk aluminum. [32-34] The nascent hydrogen atoms eventually recombine to form hydrogen gas. The steps for the first phase $NaAlH_4$ decomposition are reactions (3)–(5), (7)-(8).

$$NaAlH_4 \rightarrow NaH + AlH_3 \quad (3)$$

$$NaH + NaAlH_4 \leftrightarrow [Na_2AlH_5] \quad (4)$$

$$NaH + [Na_2AlH_5] \leftrightarrow Na_3AlH_6 \quad (5)$$

$$Na_3AlH_6 \rightarrow 3NaH + AlH_3 \quad (6)$$

$$AlH_3 \leftrightarrow Al + 3H \quad (7)$$

$$2H \leftrightarrow H_2 \quad (8)$$

The decomposition process continues in Phase 2 where thermally activated Na_3AlH_6 produces more AlH_3 and NaH. During this phase, the final solid product NaH begins to build; reactions (4) and (5) are about fully developed. AlH_3 decomposes to produce hydrogen as before. The steps for the second phase Na_3AlH_6 decomposition are reactions (6)–(8). (Note: reactions (6) and (7) are multi-step decompositions.)

The hydrogen evolution dynamics of Na_3AlH_6 are comparable to $NaAlH_4$ based on the similarity of the neat activation energies and the primary products of reaction, NaH and AlH_3. The measured activation energies for the Phase 1 evolution of hydrogen is 118.1 kJ/mol-H_2 for neat $NaAlH_4$ and for the Phase 2 evolution of hydrogen, 120 kJ/mol-H_2 for neat Na_3AlH_6. [24] The itemized steps for the sodium alanate decomposition are a combination of uni-molecular and bi-molecular reactions that, with the proper stoichiometry, sum to the overall mass balanced equations for the decomposition of sodium alanate, equations (1) and (2).

The decomposition mechanism proposed here is a kind of fugue for two sodium alanates, one following the other and both producing NaH and AlH_3 as primary products. The earlier production of NaH provides the reaction dynamics for the formation of the second alanate; the later production of NaH provides a final product; the alane provides

the evolved hydrogen gas and bulk aluminum. The literature thermodynamic and rate data make available a template for the general reaction dynamics for sodium alanate. [5,16,18,24]

3. Calculation

The calculation uses equations (3)–(10) to determine the time dependences for the various species. Equations (9) and (10) are included in the calculated evolution plots for completeness; they contribute very little to the overall dynamics.

$$[Na_2AlH_5] + NaAlH_4 \bullet \quad Na_3AlH_6 + AlH_3 \qquad (9)$$

$$[Na_2AlH_5] \bullet \quad 2NaH + AlH_3 \qquad (10)$$

The time-dependent differential equations derived from the individual mechanistic steps are simultaneously solved (5^{th} order Ruge-Kutta-Fahlberg). The resulting kinetic plots of the species describe the reported time dependence of the decomposition of $NaAlH_4$ and Na_3AlH_6. (Figure 1.) Details of the calculation are in Appendix B.

4. Discussion

The task now is to show the correlation between the calculated kinetic results and the observed dynamics reported in the literature. Several articles illustrate the action of decomposing alanates; we choose to compare global observations of decomposing sodium alanate with our derived kinetics, rather than to compare specific effects of a technique. We make two literature comparisons: the kinetic development displayed by the in-situ X-ray diffraction (XRD) data by Gross et al. [16]; and the relative phase contents for both decomposition and reformation reported by Bogdanovic et al. [26]

4.1 XRD Data Simulation

Gross et al. present in-situ X-ray diffraction data for the decomposition of neat $NaAlH_4$. [16] Repetitive XRD scans for several hours (about 7 minute intervals, 3° min^{-1}) over a small angle range that includes reflections of the major species clearly show the evolution of the decomposition. Upon reaching and holding the melt temperature (180°C), a rapid change occurs in the XRD experiment. The crystalline $NaAlH_4$ reflections disappear since it has fused. Then, immediately upon melting, an unidentified crystalline phase precipitates and the aluminum content increases rapidly. In addition, this unidentified phase X1 almost completely develops at the melt, and is the only crystalline material observed for a couple of scans. As this unidentified phase declines, the expected Na_3AlH_6 phase begins to appear. As the Na_3AlH_6 phase forms, it decomposes into NaH.

Table 1. Thermodynamic values* for $NaAlH_4$ and Na_3AlH_6 [18]

$NaAlH_4$ (s) ↔ 1/3Na_3AlH_6(s) + 2/3 Al + H_2(g)	ΔH=38.5 kJ/mol-H_2	ΔS = 125 J/mol-°K
Na_3AlH_6(s) ↔ 3NaH(s) + Al + 3/2 H_2(g)	ΔH=46.1 kJ/mol-H_2	ΔS = 123 J/mol-°K
$NaAlH_4$ (s) ↔ NaH(s) + Al + 3/2 H_2(g)	ΔH=53.8 kJ/mol-H_2	
$NaAlH_4$ (•) ↔ 1/3Na_3AlH_6(s) + 2/3Al + H_2(g)	ΔH=8.2 kJ/mol-H_2	ΔS = 59 J/mol-°K
$NaAlH_4$ (s) ↔ $NaAlH_4$ (•)	ΔH=30 kJ/mol (*Est. Number*)	
NaH(s) ↔ Na(•) +1/2H_2(g)	ΔH=57 kJ/mol (*Est. Number*)	
2NaH(s) + $NaAlH_4$(s) ↔ Na_3AlH_6(s)	ΔH~ (*-23 kJ/mol-H_2*) (*See below*)	

Estimation of the heat of reaction, ΔH, for NaH + $NaAlH_4$:

$2\ NaAlH_4 \rightarrow 2\ NaH + 2Al + 3H_2$ 3(2 x 53.8)

$2\ NaH + NaAlH_4 \rightarrow Na_3AlH_6$?

$3\ NaAlH_4 \rightarrow Na_3AlH_6 + 2Al + 3H_2$ 3 x (38.5)

$3\ (38.5 - 107.6) \approx -69$ kJ/3mol-$H_2 \approx -23$ kJ/mol-H_2

*ΔS and ΔH values have been normalized to P_o=1 atm (750 bar).

Figures 1 and 2 generally reproduce this observed kinetic evolution of species from neat $NaAlH_4$ decomposition. Figure 1 shows the calculated kinetic evolution plot of the decomposition starting with $NaAlH_4$ only; Figure 2 shows the same evolution plot but with 10% NaH added at the start. These plots clearly show the overall dynamics observed in the XRD data: $NaAlH_4$ disappears rapidly and aluminum grows in; as $[Na_2AlH_5]$ (the "unidentified" intermediate X1) decays, the Na_3AlH_6 grows in; NaH builds into the plots as Na_3AlH_6 decomposes, even though NaH also is a primary product of the $NaAlH_4$ first decomposition step. According to the proposed mechanism, this is consistent. Equations (4) and (5) are slightly exothermic (See Table 1), and as such, hold NaH to a very low concentration during Phase 1. [3,4,6,9]. NaH is not seen early on in the XRD. However, with added NaH at the start, Figure 2 demonstrates $[Na_2AlH_5]$ immediately reaches full development, as observed for the X1 unidentified phase at the melt. Based on our plot with added NaH, it appears that a burst of NaH from rapidly decomposing fused $NaAlH_4$ increases the rate of reaction (4) dramatically.

These calculated features demonstrate the kinetic equations derived from the described mechanism imitate to a large degree the observed reality of $NaAlH_4$ decomposition, even with the assumed stoichiometry of the unidentified intermediate $[Na_2AlH_5]$. This may in fact be the composition of the X1 species observed by Gross et al. [16]

4.2 Relative Species Content Simulation

Adding to the growing body of data for alanate systems, Bogdanovic et al. contribute XRD and Magic Angle Spinning solid-state NMR measurements of the relative species contents of cycled titanium-doped $NaAlH_4$. [26] For the decomposition reaction,

measurements of the sample composition were made at about one-half of the decomposition of the Phase 1 reactions, at about full decomposition of the Phase 1 reactions, at full decomposition of the Phase 2 reactions, and then at the maximum extent of reaction for rehydrogenation with and without added aluminum. The decomposition data sets are discussed in the context of the proposed mechanism. The rehydrogenation data are discussed below.

At about full decomposition of Phase 1 (equations 3-5 for our proposed mechanism), 7-mol% $NaAlH_4$, 30-mol% Na_3AlH_6, and 63-mol% aluminum make up the solid sample contents. At about one-half decomposition of Phase 1, 49-mol% $NaAlH_4$, 15-mol% Na_3AlH_6, and 36-mol% aluminum are the sample contents. [26]

The kinetic plots derived from our proposed mechanism reproduce to a great extent this measured speciation. For example, at the point $NaAlH_4$ has decreased from 100-mol% to about 7-mol% in Figure 1, Na_3AlH_6 is 29-mol%, and aluminum is 61-mol% (values adjusted for amount of NaH in calculated plots, which has continued to react when the measurement was made. See Table 2). The plot accounts for 97% of these species. When $NaAlH_4$ is about 50-mol%, Na_3AlH_6 is 10-mol%, and aluminum is 30-mol%. The plot accounts for 90% of these species. Of course, at full decomposition of Phase 2, only NaH and bulk aluminum remains. These plots do not include the titanium catalyst, signifying the dopant simply alters the rates of reaction and not the mechanism of reaction.

4.3 Rehydrogenation

With this demonstrated understanding of the decomposition mechanism for sodium alanate, a rehydrogenation mechanism begins to take shape. The mass spectrum of

Table 2. Measured and Calculated Mole %: Phase 1 Extent of Reaction

Species	Meas.*	Calc.	Adj.**
50% Phase 1			
$NaAlH_4$	49	*50*	*50*
Na_3AlH_6	15	9	10
Al	36	28	30
NaH	0	2	0
			90
100% Phase 1			
$NaAlH_4$	7	*7*	*7*
Na_3AlH_6	30	22	29
Al	63	57	61
NaH	0	12	0
			97

* Bogdonavic, et al, [26]
** Adjusted Values: During Phase 1 reactions, NaH reacts with $NaAlH_4$ when quenched to make the measurement. Values adjusted to reflect continued reaction to deplete NaH.

gaseous species formed from hydrogen adsorbed onto aluminum surfaces shows both hydrogen (H) and AlH_x (x = 2,3) desorbe at around 50°C. The predominate cracking product of the alane is H atom, not H_2. [16,33,34] For the dehydrogenation process, this simple decomposition of AlH_3 to Al and three H atoms produces hydrogen gas. This is the preferred decomposition mode of alanes on aluminum surfaces at low hydrogen coverage, [33] and corresponds with our proposed decomposition mechanism. The rehydrogenation process, however, requires high-pressure hydrogen gas, a condition that encourages the formation and desorption of alanes. [33] According to the principle of microscopic reversibility, if alanates decompose through alanes, then alanates rehydrogenate through alanes. This rehydrogenation mechanism could be as follows:

$$Al^\circ + H_2 \leftrightarrow AlH_x \ (x = 2,3) \qquad (12)$$

$$AlH_3 + NaH \leftrightarrow Na_3AlH_6 \bullet \ \bullet \ NaAlH_4 \qquad (13)$$

The high-pressure hydrogen creates the conditions for alane desorption as described. [33,34] The alane then migrates to NaH and reacts, forming both of the alanates, first

Na_3AlH_6 and then $NaAlH_4$. [16,35] Assuming both $NaAlH_4$ and Na_3AlH_6 form this way, the theoretical ratio of Na_3AlH_6 to $NaAlH_4$ should be 0.33 (i.e., all of the sodium is contained in one-third mole fraction Na_3AlH_6; then $NaAlH_4$ forms. See Appendix A). The ratio was found to be 0.27±0.03 upon rehydrogenation, not the expected 0.33. [26] The chemical stability of the two alanates appears to play a role and provides the understanding of this relative deviation.

The heat of reaction for the formation of the two alanates from hydrogen, aluminum and NaH is an approximate measure of their relative chemical stability. The ratio of the enthalpies for the reactions to form $NaAlH_4$ and Na_3AlH is 0.86 (ΔH [Na_3AlH_6] = 46.1 kJ/mol-H_2, ΔH [$NaAlH_4$] = 53.8 kJ/mol-H_2, see Table 1). As a first order approximation, $NaAlH_4$ is about 14% less stable than Na_3AlH_6 when made from the elements and NaH in the solid state. [35] The product of the theoretical maximum value (0.33) and the stability-partitioning factor (0.86) is 0.29, in good agreement with the measured value for this ratio, considering the approximation. The reaction mechanism that relies on the reaction of alanes with NaH to produce both alanates allows this calculation. This is a different scenario than proposed by Bogdanovic, where presumably metallic aluminum particles react with NaH. [26]

Adding excess aluminum upon rehydrogenation assists the reformation of sodium alanate completely back to $NaAlH_4$. [26] From a synthesis approach, and our proposed reformation mechanism, it is easy to see the added aluminum promotes the formation of mobile alanes, which attack the NaH-rich Na_3AlH_6 and form the less stable $NaAlH_4$. [35] Alane mobility also explains the facile (low temperature) segregation of bulk aluminum

after complete hydrogen desorption, and then the reformation of crystalline alanates upon rehydrogenation. [16,19]

4.4 Titanium Catalyst

The fundamental understanding of the role of the titanium dopant as a catalyst has remained at large ever since titanium facilitated the dynamics of sodium alanate. In an attempt to pin down the function, aluminum-titanium alloy phases are under investigation because of the relevance of titanium to the catalytic effect on sodium alanate cycling kinetics. [13,26,29] With the understanding acquired from the success of our proposed mechanism, and from the growing body of reaction data for $NaAlH_4$, we propose the major catalytic effect of titanium on sodium alanate kinetics appears to be the alteration of the surface of bulk aluminum with titanium-aluminum alloys, specifically $TiAl_3$. [22,26,36] The bulk aluminum surface is coincident with the decomposition and reformation mechanisms through the common intermediate species AlH_3. The bulk aluminum surface is the single location where the function of the catalyst affects both hydrogen evolution and alanate reformation. Preliminary calculation results indicate the surface of titanium-altered aluminum exhibits increased obtruding electron density, with a developed dipolar characteristic. [37] The description of the catalyzed reversible mechanism for hydrogen uptake and release presented here describes to a large extent the dynamics of the sodium alanate hydrogen storage system.

5. Conclusions

This work allows several conclusions. A simple mechanism involving NaH and AlH_3 appears to be sufficient to describe the reported dynamics for sodium alanate, catalyzed and neat, solid and fused. The alane AlH_3 plays a major role in that both the

decomposition mechanism and the reformation mechanism rely on its mobility and sorption characteristics. Moreover, since the alane is intimately associated with the bulk aluminum surface, the role of titanium as a catalyst centers on the formation of titanium-aluminum alloys that facilitate the alane formation and sorption dynamics for both decomposition and reformation mechanisms. The puzzling behavior of sodium alanates sorts itself along these mechanistic arguments.

Calculations are underway in two areas as a result of this work. We are investigating the surface property changes between bulk aluminum and aluminum with a surface layer of titanium alloy to understand the catalytic effect of the alloy. In addition, we seek a reasonable structure for the [Na_2AlH_5] intermediate that will provide an XRD spectrum similar to that reported for the X1 intermediate. [16]

"Everything should be made as simple as possible, but not simpler." [38]

Acknowledgement

This document was prepared in conjunction with work accomplished under Contract No. DE-AC09-96SR18500 with the U.S. Department of Energy.

References:

[1] "Basic Research Needs for the Hydrogen Economy", Report from the Basic Energy Sciences Workshop on Hydrogen Production, Storage, and Use, US Department of Energy, Office of Science, May 13-15, 2003. Report prepared by Argonne National Laboratory. (http://www.sc.doe.gov/bes/hydrogen.pdf)
[2] J. Block, A.P. Gray, Inorganic Chemistry, 4 (1965) 304
[3] V.V. Gavrilenko, G.A. Egorenko, L.M. Antipin, L.I. Zakharkin, Russian J. Inorg. Chem., 12 (1967) 317
[4] L.I. Zakharkin, V.V. Gavrilenko, L.M. Antipin, Yu T. Struchkov, Russian J. Inorg. Chem., 12 (1967) 607
[5] G.C. Sinke, L.C. Walker, F.L. Oetting, D.R. Stull, J. Chem. Phys., 47 (1967) 2759; J.W. Turley, H.W. Rinn, Inorg. Chem.., 8 (1969) 18.
[6] T.N. Dymova, S.I. Bakum, Russian J. Inorg. Chem., 14 (1969) 1683
[7] E.C. Ashby, B.D. James, Inorganic Chemistry 8 (1969) 2468; E.C. Ashby, P. Kobetz, Inorganic Chemistry, 5 (1966) 1615
[8] S. Aronson, F.J. Salzano, Inorganic Chemistry 8 (1969) Notes 1541
[9] J.A. Dilts, E.C. Ashby, Inorganic Chemistry, 11 (1972) 1230
[10] V.K. Bel'skii, B.M. Bulychev, A.V. Golubeva, Russian J. Inorg. Chemistry 28 (1983) 1528
[11] J.P. Bastide, P. Claudy, J.M. Letoffe, J. El Hajri, Inorg. Chimica Acta, 141 (1988) 11-12
[12] B. Bogdanovic, M. Schwickardi, J. Alloys Comp. 253-254 (1997) 1-9
[13] A.J. Maeland, B. Hauback, H. Fjellvag, M. Sorby, Int. J. Hydrogen Energy 24 (1999) 163-168
[14] R. Zidan, S. Takara, A. Hee, C. Jensen, J. Alloys Comp. 285 (1999) 119-122.
[15] C. Jensen, R. Zidan, N. Mariels, A. Hee, C. Hagen, Int. J. Hydrogen Energy 24 (1999) 461-465
[16] K.J. Gross, S. Guthrie, S. Takara, G. Thomas, J. Alloys Comp. 297 (2000) 270-281
[17] A. Zaluska, L. Zaluski, J.O. Strom-Olsen, J .Alloys Comp. 298 (2000) 125-134
[18] B. Bogdanovic, R.A. Brand, A. Marjanovic, M. Schwickardi, J. Tolle, J. Alloys Comp. 302 (2000) 36-58
[19] K.J. Gross, G.J. Thomas, C.M. Jensen, J. Alloys Comp. 330-332 (2002) 683-690
[20] K.J. Gross, G. Sandrock, G.J. Thomas, J. Alloys Comp. 330-332 (2002) 691-695
[21] G. Sandrock, K. Gross, G. Thomas, C. Jensen, D. Meeker, S. Takara, J. Alloys Comp. 330-332 (2002) 696-701
[22] G.J. Thomas, K.J. Gross, N.Y.C. Yang, C. Jensen, J. Alloys Comp. 330-332 (2002) 702-707
[23] G.P. Meisner, G.G. Tibbetts, F.E. Pinderton, C.H. Olk, M.P. Balogh, J. Alloys Comp. 337 (2002) 254-263
[24] G. Sandrock, K. Gross, G. Thomas, J. Alloys Comp. 339 (2002) 299-308
[25] M.P. Galogh, G.G. Tibbetts, F.E. Pinderton, G.P. Meisner, C.H. Olk, J. Alloys Comp. 350 (2003) 136-144
[26] B. Bogdanovic, M. Felderhoff, M. Germann, M. Hartel, A. Pommerin, F. Sschuth, C. Weidenthaler, B. Zibrowius, J. Alloys Comp. 350 (2003) 246-255
[27] E.H. Majzoub, K.J. Gross, J. Alloys Comp. 356-357 (2003) 363-367
[28] D.L. Anton, J. Alloys Comp. 356-357 (2003) 400-404
[29] K.J. Gross, E.H. Majzoub, S.W. Spangler, J. Alloys Comp. 356-357 (2003) 423-428
[30] S.M. Opalka, D.L. Anton, J. Alloys Comp. 356-357 (2003) 486-489
[31] The room temperature decomposition of doped $NaAlH_4$ occurs at a very low rate. See reference [24].
[32] P. Breisacher and B. Siegel, J. Amer. Chem. Soc., 86 (1964) 5035.
[33] A. Winkler, Ch. Resch, K.D. Rendulic, J. Chem. Phys. 95 (10) (1991) 7682.
[34] E.P. Go, K. Thukermer, J.E. Reutt-Robey, Surface Science 437 (1999) 377 – 385.
[35] Initially, Na_3AlH_6 is found in the direct synthesis of $NaAlH_4$ from the elements sodium, aluminum and hydrogen. See reference [4].
[36] J.A. Jegier, W.L. Gladfelter, Coord. Chem. Reviews, 206-207 (2000) 631-650.
[37] J. Becnel, R. T. Walters, work in progress.
[37] A. Einstein quoted in *Newsweek* 93 (1979).

Appendix A.

Starting with "n" moles of $NaAlH_4$, the full decomposition and reformation mechanism is as follows.

Decomposition:

$$n\ NaAlH_4 \bullet\ \bullet\ \ n\ NaH + n\ Al^\circ \qquad (A1)$$

Reformation:

$$n\ Al^\circ + H_2\ (\text{Hi Press}) \bullet\ \ n\ AlH_3 \qquad (A2)$$

$$n\ AlH_3 + n\ NaH \bullet\ \ 1/3n\ Na_3AlH_6 + 2/3n\ AlH_3 \qquad (A3)$$

$$1/3n\ Na_3AlH_6 + 2/3n\ AlH_3 \leftrightarrow n\ NaAlH_4 \qquad (A4)$$

n moles of NaH and Al result from the decomposition of n moles of $NaAlH_4$. Upon reformation, n moles of AlH_3 react with the n moles of NaH and form 1/3n moles of Na_3AlH_6; the Na_3AlH_6 contains the mass balance of the sodium. With the continuance of the high pressure of hydrogen to stabilize AlH_3, equilibrium between the two alanates obtains. At equilibrium, the ratio of Na_3AlH_6 to $NaAlH_4$ is 0.33, all things being equal.

Appendix B. Details of Calculation Method

The reaction has been modeled as a series of elementary reactions. While not all of the essential reaction steps presented above are elementary, they have been broken down into "reasonable" elementary reactions for the purpose of producing a defendable model. For example, the reaction

$$Na_3AlH_6 \leftrightarrow 3\ NaH + AlH_3 \qquad (B1)$$

Has been broken down into three steps, first forming an alane and a complex of sodium hydrides, which then breaks down sequentially into individual sodium hydride monomers:

$$Na_3AlH_6 \leftrightarrow [Na_3H_3] + AlH_3 \qquad (B2)$$

$$[Na_3H_3] \leftrightarrow [Na_2H_2] + NaH \qquad (B3)$$

$$[Na_2H_2] \leftrightarrow 2\ NaH \qquad (B4)$$

Each of the reactions (B2) – (B4) can be assumed to be an elementary reaction. By choosing fast forward and reverse reaction rates for B3 and B4, the limiting step becomes B2. This case is roughly equivalent to modeling the reaction network only using reaction B1. As none of the intermediates in B3 or B4 are seen, it is reasonable to assume that the rates for these reactions are fast. Therefore, it is equivalent to use elementary reaction B2, B3 and B4 where B3 and B4 have fast reaction rates, in place of reaction B1. For simplicity in modeling and to reduce the number of degrees of freedom, the reaction rates of B3 and B4 have been kept at least one order of magnitude higher than B2. Additionally, for reasons of symmetry, the decomposition of the $[Na_2AlH_5]$ species has been added to parallel the decomposition of both $NaAlH_4$ and Na_3AlH_6.

Similarly, the alane decomposition reaction has been decomposed into a series of three sequential decomposition reactions.

$AlH_3 \leftrightarrow AlH_2 + H$ (B5)
$AlH_2 \leftrightarrow AlH + H$ (B6)
$AlH \leftrightarrow Al + H$ (B7)

Thus we now have a network of 12 species in 12 elementary reactions:

1. $NaAlH_4 \leftrightarrow NaH + AlH_3$
2. $NaAlH_4 + NaH \leftrightarrow [Na_2AlH_5]$
3. $[Na_2AlH_5] + NaH \leftrightarrow Na_3AlH_6$
4. $NaAlH_4 + [Na_2AlH_5] \leftrightarrow Na_3AlH_6 + AlH_3$
5. $[Na_2AlH_5] \leftrightarrow [Na_2H_2] + AlH_3$
6. $Na_3AlH_6 \leftrightarrow [Na_3H_3] + AlH_3$
7. $[Na_3H_3] \leftrightarrow [Na_2H_2] + NaH$
8. $[Na_2H_2] \leftrightarrow 2\ NaH$
9. $AlH_3 \leftrightarrow AlH_2 + H$
10. $AlH_2 \leftrightarrow AlH + H$
11. $AlH \leftrightarrow Al + H$
12. $2H \leftrightarrow H_2$

The individual differential equations for each species *i* is represented in the classic formulation as

$$\frac{\partial C_i}{\partial t} = \sum_{k=1}^{T}\left[\left(P_{(k,i)} - R_{(k,i)}\right)\left(F_k \prod_{j=1}^{S}\left[C_j\right]^{R_{(k,j)}} - B_k \prod_{j=1}^{S}\left[C_j\right]^{P_{(k,j)}}\right)\right]$$

where

t = time
C_i = the concentration of species *i* at time t
T = the total number of reactions
S = the total number of species
$P_{(k,i)}$ = the coefficient of species *i* in the product (rhs) of reaction t
$R_{(k,j)}$ = the coefficient of species *i* in the reactant (lhs) of reaction t
F_k = the forward reaction rate of reaction t
B_k = the reverse reaction rate of reaction t

The reaction network was modeled using a time step adaptive fifth order Runge-Kutta-Fehlberg method. [A] The time adaptive behavior allows the model to take smaller steps when the variables are changing rapidly, and larger steps when the variables are changing slowly. This approach allowed the model to be readily changed, so that different decomposition alternatives could be tested. In particular, it was found that using

the lumped non-elementary decompositions produced the same qualitative results as using the multiple elementary reactions. Since there was a slight difference in time-dependant behavior of the two systems, the results presented here are those produced with the network of elementary reactions.

To simulate the removal of hydrogen gas from the system, the reaction rate of the reverse reaction for the formation of hydrogen gas was set to a very low value. Additionally, the equilibrium constant of the initial decomposition of $NaAlH_4$ must strongly favor the formation of $NaAlH_4$ rather than NaH, therefore the forward and reverse reaction rates of that reaction are set accordingly.

When beginning with a starting composition of pure $NaAlH_4$, the reaction takes a substantial amount of time to start, as the concentration of NaH must increase to a level where the reactions producing Na_3AlH_6 begin to proceed at a reasonable rate.

[A] Press, W.H., et al, *Numerical Recipes in C: The Art of Scientic Computing*, 2nd Ed., Cambridge University Press, 1992, ISBN 0-521-43108-5.

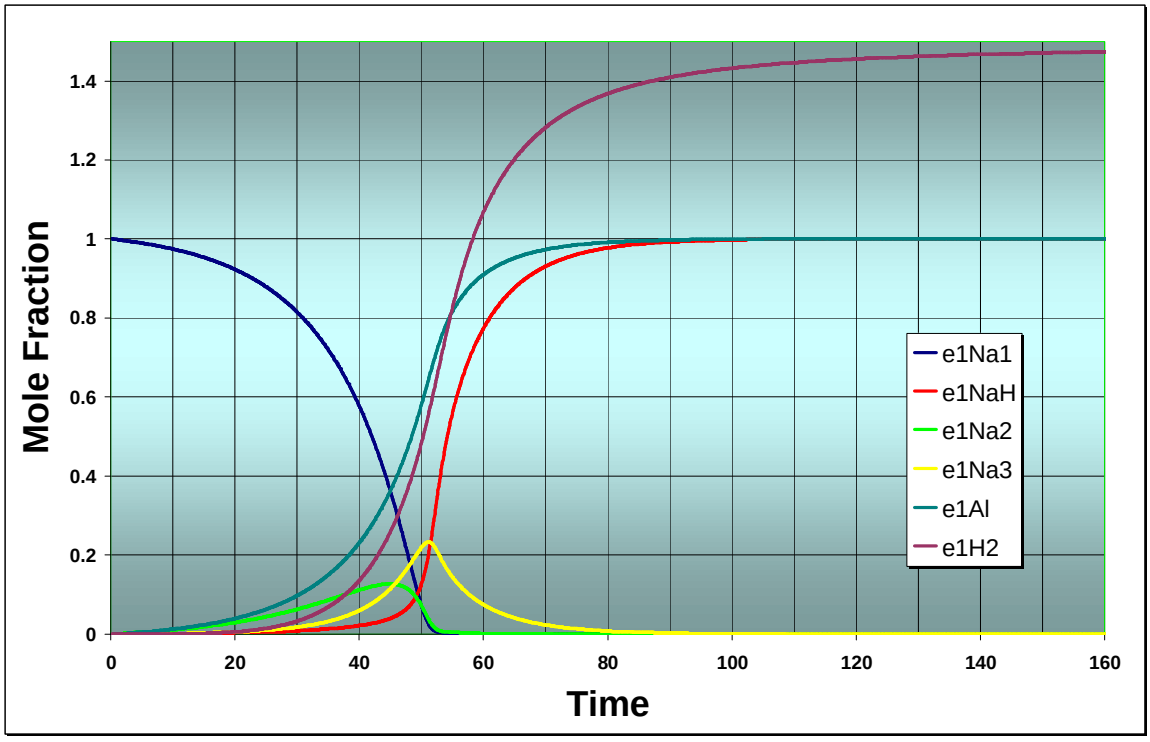

Figure 1. Kinetic evolution of Species.

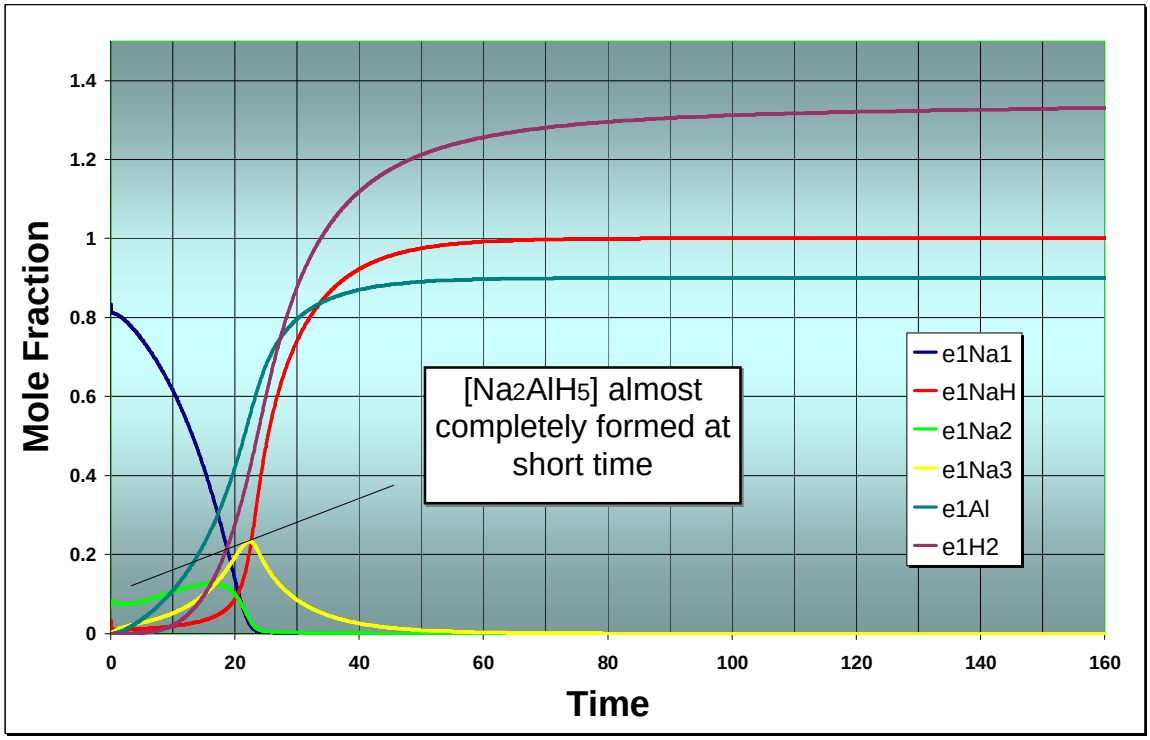

Figure 2. Added 10% NaH at start.